Nonlinear diffusion filters without parameters for image segmentation

Carlos Platero, Javier Sanguino, and Olga Velasco

Applied Bioengineering Group, Polytechnic University of Madrid, Spain

Abstract. Nonlinear diffusion filtering seeks to improve images qualitatively by removing noise while preserving details and even enhancing edges. However, well known implementations are sensitive to parameters which are necessarily tuned to sharpen a narrow range of edge slopes. In this work, we have selected a nonlinear diffusion filter without control parameters. It has been guided searching the optimum balance between time performance and resulting quality suitable for automatic segmentation tasks. Using a semi-implicit numerical scheme, we have determined the relationship between the slope range to sharpen and the diffusion time. It has also been selected the diffusivity with optimum performances. Several diffusion filters have been applied to noisy computed tomography images and evaluated for their suitability to the medical image segmentation. Experimental results show that our proposal of filter performs quite well in relation to others.

Key words: nonlinear diffusion filter, segmentation, 3D medical image

1 Introduction

For improving the segmentation task, a pre-processing filter has to be applied to the original image in order to remove the noise from homogeneous area while keeping clear and sharp the edges. In the field of image processing, several filtering methods are available for this purpose[1]. Convolutions and rank filters (median filter, mean filter, etc.) reduce the image noise, but they did not preserve the details and tended to blur the edges. Nonlinear filters smooth the noise while maintaining clear edges. We have selected a nonlinear diffusion filter without control parameters, searching the optimum balance between time performance and resulting quality suitable for automatic segmentation tasks.

The paper is organized as follows: in section 2, we explain our theoretical framework, which analyzes a diffusivity without tuning parameters and its properties. In section 3, we show the numerical algorithm for nonlinear diffusion and determine the time needed for area smoothing and edge enhancement purposes. Finally, in section 4, some diffusion filters are compared on computed tomography images with a rich variety of features and edge types but also with a significant noise level. Experiments demonstrate that our proposal of filter performs quite well compared to others.

2 Nonlinear diffusion without control parameters

Starting with an initial image $u_0 : \Omega \to \mathbb{R}$ defined over a domain $\Omega \subset \mathbb{R}^m$, another image $u(\boldsymbol{x})$ is obtained as the solution of a nonlinear diffusion equation with initial and Neumann boundary conditions:

$$u_t = \operatorname{div}\left(g(\|\nabla u\|)\,\nabla u\right), \quad \boldsymbol{x} \in \Omega, \quad t > 0, \tag{1}$$

with $u(\boldsymbol{x}, 0) = u_0(\boldsymbol{x})$ when $\boldsymbol{x} \in \Omega$ as initial condition and $u_{\boldsymbol{n}} = 0$ when $\boldsymbol{x} \in \partial\Omega$ as boundary condition, with $g(\|\nabla u\|)$ further representing *diffusivity*. We have chosen a diffusivity which balances between sharpen edges over a wide range of selected slopes and reduce noise conservatively with dissipation along feature boundaries. Specifically, the range of sharpned edge slopes is widened as backward diffusion normal to level sets is balanced with forward diffusion tangent to level set. Our family of diffusivity, as in the TV flow case, is free from parameters, but allows backward diffusion along the gradient direction and it is therefore edge enhancing [2][3]:

$$g(\|\nabla u\|) = \frac{1}{\|\nabla u\|^p},\ p > 1. \tag{2}$$

The diffusion properties of these filters can be showed when set out in a new orthonormal basis in which one of the axes is determined by the gradient vector $\eta = \nabla u/\|\nabla u\|$ where $\|\nabla u\| \neq 0$, which together with ξ and ζ form the curve/surface at a level perpendicular to η[4]:

$$u_t = g(\|\nabla u\|)\,(u_{\xi\xi} + u_{\zeta\zeta}) + [\,g(\|\nabla u\|) + g'(\|\nabla u\|) \cdot \|\nabla u\|\,]\,u_{\eta\eta} \tag{3}$$

where $u_{\eta\eta}$ represents the second derivative of u in the direction of η. Thus, tangential diffusion is always forward since $g(\|\nabla u\|) > 0$ and normal diffusion is always backward since

$$[g(\|\nabla u\|) + g'(\|\nabla u\|) \cdot \|\nabla u\|\,] = \frac{1-p}{\|\nabla u\|} < 0. \tag{4}$$

Continuum level analysis of smooth images shows that diffusivity should be chosen so edge slopes with $\|u_\eta\| \leq \alpha_{th}$ must be blurred and edges slopes with $\|u_\eta\| > \alpha_{th}$ must be heightened at a locally maximal rate which leads to sharpening and avoiding staircasing, where α_{th} is the threshold slope on which enhancement is achieved. Open questions are: 1) what is the optimum value of p? and 2) given a particular value of α_{th}, what is the diffusion time required for the selected edge enhancement task? In the continuum domain, this approach gives rise to an ill-posed problem[5, 6]. However, in the discrete scheme, under certain data conditions, we can obtain the convergent solutions as referred to in [5]. For more detail see [7].

As we stated above, for enhancement process the $u_{\eta\eta}$ coefficient left to be positive, so this implies that differential operator in (3), loses the necessary conditions for a well-posed problem. An introduction about this topic can be

found in a classical Weickert's paper [8] and the references therein cited. However with the Perona-Malik filter [9] in (1) we also get an ill-posed problem, but discretization has a stabilizing effect over this equation [7]. We follow this pattern for the proposed diffusivity (2). Therefore, we apply the Method of Lines to transform the original equation (1) into a semi-discrete problem and a well-posed system of ordinary differential equations using the scale-space framework proposed by Weickert [7]. This also implies some kind of regularization in order to avoid unbounded diffusivity (2), when the gradient tends to 0, and hence to keep the system of ordinary differential equations continuously differentiable as function in u.

With this aim, we use an approximation on finite differences based on the average distance between pixels, which subsequently gives rise to an autonomous system of ordinary differential equations:

$$\dot{u}_i(t) = h^{p-2}\left[\frac{u_{i+1}(t)-u_i(t)}{|u_{i+1}(t)-u_i(t)|^p} - \frac{u_i(t)-u_{i-1}(t)}{|u_i(t)-u_{i-1}(t)|^p}\right] \tag{5}$$

with $h = \Delta x, i = 2,\ldots,n-1$. On carrying out the operation we get an autonomous matrix ordinary differential expression of the type $\frac{d\boldsymbol{U}}{dt}(t) = \boldsymbol{f}(\boldsymbol{U}(t)) = A(\boldsymbol{U}(t))\,\boldsymbol{U}(t)$. The generalisation to highest dimension is straightforward [10].

3 Numerical methods

Numerical methods have a decisive effect on the outcome of nonlinear diffusion regarding both quality and computation speed. With spatial discretization, the differential equation has been ported to the pixel grid. An explicit Euler method can be computed by an iterative scheme. For stability it has been assumed that diffusivity is limited, however, edge enhancing flow causes unbounded diffusivity when the gradient tends to 0. A popular solution to this problem is the regularization of the diffusivity by a small positive constant ε, taking $g_\varepsilon(s) = \frac{1}{(s+\varepsilon)^p} \leq \frac{1}{\varepsilon^p}$ with $s \geq 0$, hence $g_\varepsilon \to g$ when $\varepsilon \to 0$. The regularization limits the diffusivity and hence the explicit scheme becomes very slow. The stability condition on the time step size can be lifted with a semi-implicit scheme. With this aim, spatial discretization is accomplished with finite difference and the temporal discretization is accomplished with semi-implicit time stepping. All pixels are assumed to have unit aspect ratios and width h and the kth time level is $t = k\tau$,

$$\frac{u_i^{k+1}-u_i^k}{\tau} = h^{p-2}\left[\frac{u_{i+1}^{k+1}-u_i^{k+1}}{|u_{i+1}^k-u_i^k|^p} - \frac{u_i^{k+1}-u_{i-1}^{k+1}}{|u_i^k-u_{i-1}^k|^p}\right]. \tag{6}$$

Using matrix-vector notation, it results an inversion matrix that has to be solved at each iteration:

$$(I - \tau A(U^k))U^{k+1} = U^k \tag{7}$$

where I is the identity matrix and $A(U^k)$ is a matrix of the same size, with the following entries:

$$a_{ij} = \begin{cases} g_{i\sim j}\, h^{-2} & \text{if } j \in N(i) \\ -\sum_{l\in N(i)} g_{i\sim l}\, h^{-2} & \text{if } j = i \\ 0 & \text{otherwise.} \end{cases} \tag{8}$$

Here, $g_{i\sim j}$ denotes the diffusivity between the pixel i and j, *N(i)* are the neighbors of pixel i. The matrix $(I - \tau A)$ is a sparse, positive definite and diagonally dominant matrix. Such a tridiagonal matrix can be solved efficiently with the Thomas algorithm. For its implementation in the scope of nonlinear diffusion see [10].

The gray evolution of a pixel depends on the whole of the pixels. For simplification, it would be interesting to observe the interaction with only three pixels within the established dynamic. Applying the semi-implicit Euler method on three pixels, the matrix is inverted giving the expression

$$\begin{bmatrix} u_1^{k+1} \\ u_2^{k+1} \\ u_3^{k+1} \end{bmatrix} = \frac{1}{d}\mathbf{B} \begin{bmatrix} u_1^{k} \\ u_2^{k} \\ u_3^{k} \end{bmatrix} \tag{9}$$

with

$$\mathbf{B} = \begin{bmatrix} \alpha^p\beta^p + 2r\alpha^p + r\beta^p + r^2 & r(\beta^p + r) & r^2 \\ r(\beta^p + r) & \alpha^p\beta^p + r\alpha^p + r\beta^p + r^2 & r(\alpha^p + r) \\ r^2 & r(\alpha^p + r) & \alpha^p\beta^p + r\alpha^p + 2r\beta^p + r^2 \end{bmatrix} \tag{10}$$

where $\alpha = |u_2^k - u_1^k| \neq 0$, $\beta = |u_3^k - u_2^k| \neq 0$, $r = \tau\, h^{p-2}$ and $d = \alpha^p\beta^p + 2r\alpha^p + 2r\beta^p + 3r^2$. For initial arbitrary value of the 3-pixels, and a finite time, the matrix coefficients are all equal to 1/3. It confirms the stability properties for $r > 0$. However, the issue lies in how to determine the nonlinear diffusion time so that it produces diffusion between the low gradient module pixels without transferring diffusion to the pixels that have a high value of the gradient module. Without loss of overall applicability, in (9) it is imposed $\alpha \gg \beta$, so as to spread forward diffusion between pixels 2 and 3 while keeping the value of the pixel 1. This evolution means that the matrix (9) tends to be $\begin{bmatrix} 1 & 0 & 0 \\ 0 & 1/2 & 1/2 \\ 0 & 1/2 & 1/2 \end{bmatrix}$, which forces $r < 2\alpha^p$. This inequality has been used to determinate the balance between forward and backward diffusion. It has been observed experimentally that this conclusion can be extended to n-pixels [11], obtaining as optimum value $p = 3$. For $h = 1$, we obtained the following expression for the time step:

$$\tau = \frac{\alpha_{th}^p}{5 \cdot n_{iter}} \tag{11}$$

where n_{iter} denotes the number of iterations (at least four iterations) and α_{th} is the absolute value of the difference between pixels, this being the slope threshold

on which enhancement is achieved. Extension to a higher dimension is carried out by applying AOS (Additive Operator Splitting) [10]. Moreover, the numerical method allows parallel and distributed computing.

4 Computational results

In order to show the performance of our proposal, it has been compared to Gauss ($p = 0$), TV ($p = 1$) and BFB ($p = 2$)[3] filters. In all cases, the time step was calculated by (11) and a semi-implicit scheme was implemented following (7). The filters have been applied over CT images for liver segmentation task. The images were taken from [12]. It is a training data set that includes both images and binary masks of the segmentations of the structures of interest, produced by human experts. There are 20 CT images. The proposed procedure is to apply the same segmentation algorithm over filtering images. The following two metrics have been commonly used to evaluate the quality of segmentation:

1. Volume overlap m_1:

$$m_1 = \left(1 - \frac{Vol_{seg} \bigcap Vol_{ref}}{Vol_{seg} \bigcup Vol_{ref}}\right) \times 100\% \tag{12}$$

   where Vol_{seg} denotes segmented volume. Vol_{ref} denotes reference volume.
2. Relative absolute volume difference m_2

$$m_2 = \frac{|Vol_{seg} - Vol_{ref}|}{Vol_{ref}} \times 100\% \tag{13}$$

To test the approaches, we apply a simple threshold technique. It uses gray level data, in order to validate the proposed image processing technique. We assume that the liver density function follows a normal, $N(\mu_{liver}, \sigma^2_{liver})$[13]. The estimation of the gaussian parameters are obtained through histogram analysis. The two thresholds for the liver have been determined by two offsets from liver mean based on the standard deviation of the gray level of the liver. Figure 1 shows the original CT and its processed images. It also depicts the contour of the manual segmentation and the image histograms. The table summarizes the experimental results. For all experiments were used the following values: $n_{iter} = 5, \alpha_{th} = 70HU, \varepsilon = 0.35HU$(HU $\equiv$ Hounsfield Units). Firstly, it is observed that the numerical method used is a conservative procedure. Independent of the filter type, it is noted that $\hat{\mu}_{liver}$ remains almost constant. Secondly, the $\hat{\sigma}_{liver}$ decreases with increasing value of p. This means removing the noise from homogenous areas while keeping clear and sharp edges. Finally, the segmentation error measures, m_1 and m_2, show a downward trend with increasing value of p. We have seen that the increase of p inhibits the staircase effect but also gives rise to a reduction in the signal dynamic range. Furthermore, the validity of equation (11) is based on the approximation between the model and numerical scheme and on which basis we conclude that a compromise value should be $p = 3$. Experiments demonstrate that our proposal of filter performs quite well in relation to others.

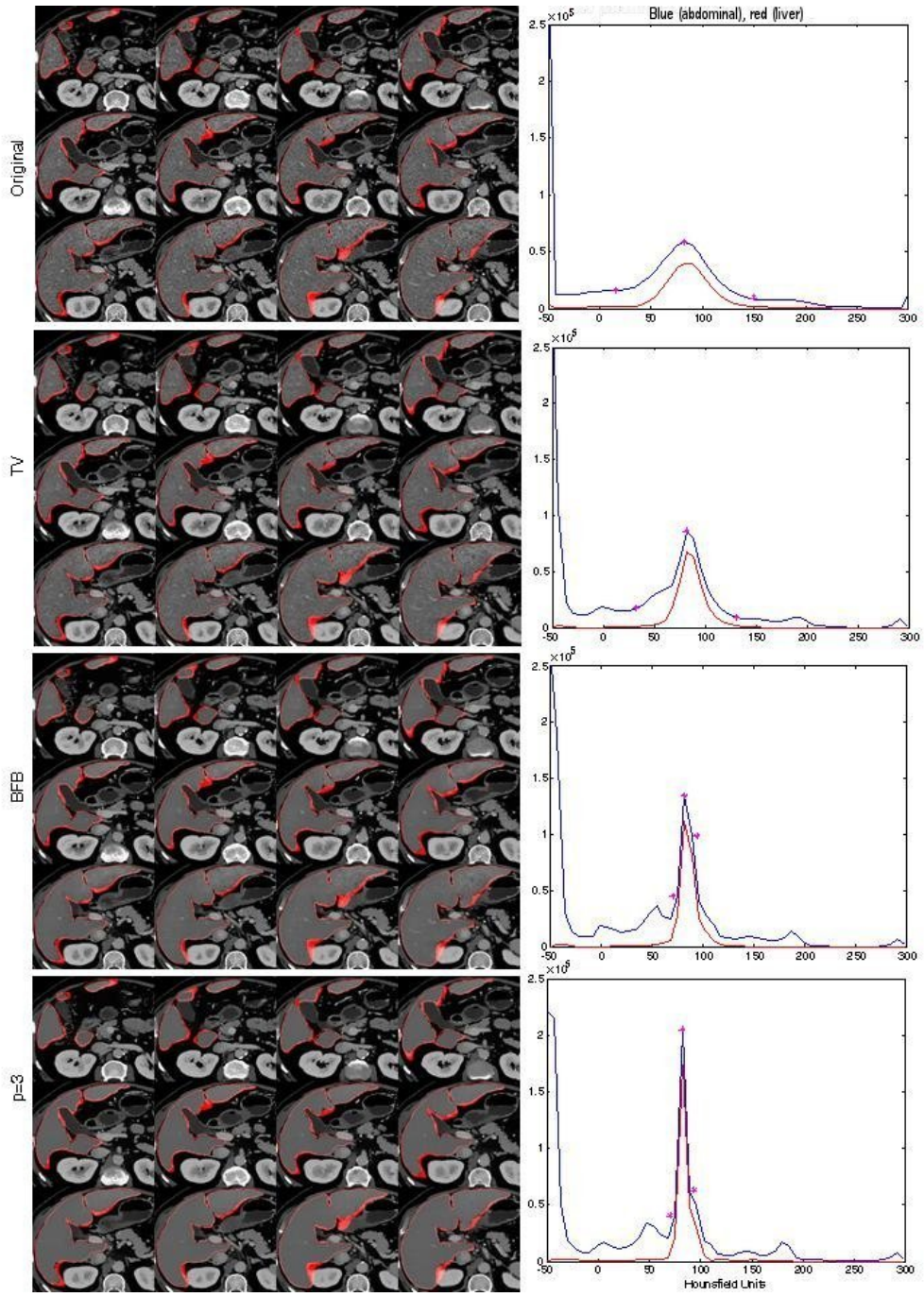

Fig. 1. Some slices over abdominal CT and their histograms a)Original, b)TV, c)BFB, d)$p = 3$

Table 1. Experimental results

	$\hat{\mu}_{liver}\,(HU)$			$\hat{\sigma}_{liver}\,(HU)$			$m_1\,(\%)$			$m_2\,(\%)$		
Type	min	mean	max	min	mean	max	min	mean	max	min	mean	max
Original	83	123	181	9.3	25.3	56.0	34.9	42.1	55.3	38.0	57.8	88.2
Gauss	83	125	181	11.7	22.3	46.6	27.4	42.3	78.1	30.3	52.6	70.6
TV	82	126	180	9.2	19.1	39.6	23.1	35.3	42.9	24.6	43.3	65.8
BFB	82	126	180	4.6	14.8	32	16.5	29.6	42.9	16.8	34.3	60.1
$p = 3$	82	126	187	4.6	9.1	21	9.3	22.4	34.3	9.6	23.7	36.5

5 Conclusions

A new nonlinear diffusion filter has been developed, which sharpens edges over a wide range of slopes and reduce noise conservatively with dissipation along homogeneous regions. It can be implemented efficiently and absolutely stable with a semi-implicit scheme and ε-regularization. Based on the discrete evolution of three pixels, we have determined the diffusion time required for the edge enhancement from a predetermined threshold. So, edge slopes below the threshold must be blurred and those above the threshold should be sharpened and trying to avoid staircase effect. Using the given time step, some diffusion filters are compared to computed tomography images for segmentation tasks. Experiments demonstrate that our proposal of filter performs quite well compared to others.

References

1. Buades, A., Coll, B., and Morel, J. M., A review of image denoising algorithms with a new one. Multiscale Modeling & Simulation, 4:490–530, 2005.
2. Tsurkov, V. I., An analytical model of edge protection under noise suppression by anisotropic diffusion. Journal of Computer and Systems Sciences International, 39(3):437–440, 2000.
3. Keeling, S.L. and Stollberger, R., Nonlinear anisotropic diffusion filters for wide range edge sharpening. Inverse Problems, 18:175–190, 2002
4. Teboul, S., Blanc-Feraud, L., Aubert, G., and Barlaud, M., Variational approach for edge-preserving regularization using couple pdes. IEEE Trasanctions on Image Processing, 7:387–397, 1998.
5. Catte, F., Lions, P. L., Morel, J. M., and Coll, T., Image selective smoothing and edge detection by nonlinear diffusion. SIAM Journal on Applied Mathematics, 29(1):182–193, 1992.
6. Kichenassamy, S., The perona-malik paradox. SIAM Journal on Applied Mathematics, 57(5):1328–1342, 1997.
7. Weickert, J. and Benhamouda, B., A semidiscrete nonlinear scale-space theory and its relation to the perona-malik paradox. Advances in Computer Vision, pages 1–10,1997.
8. Weickert, J., A Review of Nonlinear Diffusion Filtering Lecture Notes in Computer Science, Vol. 1252, Springer, Berlin, pages 3–28,1997.
9. Perona, P. Malik, J., Scale space and edge detection using anisotropic dffusion. IEEE Transaction on Pattern Analysis and Mach. Intell (12):629–639, 1990.

10. Weickert, J., ter Haar Romeny, B., and Viergever, M. A., Efficient and reliable schemes for nonlinear diffusion filtering. IEEE Trasanctions on Image Processing, 7(3):398–410, 1998.
11. Platero, C., Sanguino, J., Tobar, M.C, Poncela, J.M., Asensio, G., Analytical Approximations for Nonlinear Diffusion Time in Multiscale Edge Enhancement. International Conference on Computer Vision Theory and Applications (VISAPP 2009). 5- 8 February, 2009 Lisboa, Portugal
12. 3D Segmentation in the Clinic: A Grand Challenge I - Liver Segmentation, `http://sliver07.isi.uu.nl/`
13. Freiman, M. and Eliassaf, O. and Taieb, Y. and Joskowicz, L. and Azraq, Y. and Sosna, J., An iterative Bayesian approach for nearly automatic liver segmentation: algorithm and validation. International Journal of Computer Assisted Radiology and Surgery, 3(5):439–446, 2008.